River Flow 2004

Chapter · January 2004

CITATIONS
0

READS
110

5 authors, including:

Mouldi Ben Meftah
Polytechnic University of Bari
126 PUBLICATIONS **1,023** CITATIONS
SEE PROFILE

Peter Davies
University of Dundee
168 PUBLICATIONS **3,146** CITATIONS
SEE PROFILE

Daniela Malcangio
Polytechnic University of Bari
81 PUBLICATIONS **466** CITATIONS
SEE PROFILE

Michele Mossa
Polytechnic University of Bari
395 PUBLICATIONS **3,573** CITATIONS
SEE PROFILE

Turbulence of vertical round buoyant jets in a cross flow

M. Ben Meftah & A. Petrillo
Water Engineering and Chemistry Department, Technical University of Bari, Italy

P.A. Davies
Civil Engineering Department, University of Dundee, United Kingdom

D. Malcangio & M. Mossa
Civil and Environmental Engineering Department, Technical University of Bari, Italy

ABSTRACT: The paper looks at a vertical round buoyant jet issued in a cross flow and investigates the effect of turbulence in the cross flow upon the structure of the jet. This general problem of the influence of ambient turbulence has been investigated for the case of cross flow turbulence associated with flow over a rough bottom boundary. The results of laboratory investigations of this problem are described and it is shown that the influence of the roughness of the bottom surface is manifested by significant modifications to the buoyant jet trajectory (as compared to the smooth boundary reference case). Preliminary attempts to quantify and parameterize these modifications are presented.

1 INTRODUCTION

One crucial problem in hydraulic engineering concerns the dilution of turbulent thermal discharges in a cross flow. The effects of cross flow turbulence (generated, as in this case, by the presence of a rough bottom boundary) upon the structure of the discharge flow is an important aspect of this problem. The study of a heated water discharge in the form of a turbulent buoyant jet into a channel with a flat bottom and with a cross current is well established in the literature (*e.g.* Lee, 1984; Il Won Seo *et al*., 2001; Young Do Kim *et al*., 2002). The flow dynamics of the thermal discharge in the near field are governed purely by the momentum source represented by the high velocity injection. In the far field, instead, mixing is governed by ambient currents and stratification. Moreover, processes at the air-water interface, such as heat exchange towards the atmosphere and wind stress, can further affect the heat distribution. As regards the ambient turbulence, the visualization study of Grass *et al*. (1991) revealed that powerful vortical structures with a general horseshoe-type configuration occur over smooth surfaces as well as in the turbulent boundary layer near rough walls and that they are similarly linked to bursting events in both the smooth and rough bed cases. The nature of coherent structures and their processes of development over rough surfaces, therefore, appear to be similar to those originating over smooth walls. Furthermore, Grass *et al*. (1991) and Grass & Mansour-Tehrani (1996) observed that a remarkable feature of the rough wall flow is its apparent ability to order itself very rapidly in a small vertical distance above the tops of the roughness elements. Their measurements indicated that for fully rough wall conditions, the near-wall turbulence structures are directly proportional to the bed roughness size for geometrically similar roughness elements and the packing used in their tests.

In order to clarify the dependence of the buoyant jet upon the background turbulence and to improve knowledge of the physical processes that determine its dilution, an experimental study was conducted. Localized background turbulence was generated within the ambient flow by means of two different corrugated plastic surfaces of known "wavelength" λ and "amplitude" ε, fixed at the bottom of a rectangular channel. During this experimental work, the characteristics of the turbulence field produced in the surrounding flow by particular combinations of λ and ε were analyzed, with the aim of finding a typical characteristic length scale of the turbulent eddies associated with flow over the rough boundary and its effect upon the structure of the buoyant jet. Since the study consisted of a three-dimensional buoyant jet interacting with a three-dimensional "patch" of shear turbulence, measurements of velocity and temperature fields were assessed at different vertical levels to obtain the spatial structure of the temperature and the velocity profile of the cross flow. Such an approach required a long time for each run, especially because relevant differences were observed at a distance of mms, and accurate and appropriate techniques to collect data, as described below were necessary.

For each configuration, the objectives of the experiments were (i) to compare the mixing of a buoy-

ant jet discharged into a cross flow with a smooth and rough boundary, (ii) to identify a distortion of the jet structure by the presence of the background turbulence generated by the rough bottom and (iii) to quantify this distortion and parameterize it in terms of buoyant jet and corrugated surfaces characteristics.

2 EXPERIMENTAL WORK

2.1 *Experimental set-up*

The laboratory model was constructed in the Coastal Engineering Laboratory of the Technical University, Bari, Italy (Fig. 1). The system consists of a rectangular steel channel 15 m long, 4 m wide and 0.4 m deep, with lateral walls and base made of transparent glass material (Saint Gobain), 15 mm tick. To create a current inside the channel a closed hydraulic circuit was constructed. The fresh water at ambient temperature was supplied from a big metallic tank downstream by a Flygt centrifugal electro-pump, which sucked the water into a steel pipe with diameter 200 mm and then discharged the same water into the upstream steel tank. Into the upstream tank a side-channel spillway with adjustable height was fitted, being made from different plates mounted together. The water that overflowed was directed into a pipe like the one for the water supply and parallel to it, with a 250 mm diameter and finally discharged into the tank downstream of the channel. Two different electromagnetic flow meters were mounted on the two parallel pipes described above in order to measure the flow rate in the channel as the difference of the two discharge measurements. The free surface level of the water into the channel, H_a, was maintained at a constant level with a depth of 26 cm for all of the experiments, to ensure that the discharge into the channel was constant.

Figure 1. A view of the channel.

The second part of the laboratory model consisted of a buoyant jet thermal-hydraulic system. The discharged heated water generating the turbulent buoyant jet was pumped into the channel through a round steel tube mounted at the bottom of the channel and within the central longitudinal section. The tube was mounted vertically and it passed through the glass base. The source diameter D = 5.0 mm of the jet was chosen to satisfy different conditions. Firstly, in all cases to ensure that the jet was fully turbulent, *i.e*. to have the Reynolds number *Re,* defined for a round jet as $Re = 4Q_0/\pi Dv$, with v the kinematic viscosity of the fluid and Q_0 the source discharge, sufficiently high (Re > 2000).
Secondly, the value of D was fixed taking into consideration the length scale l_M, defined in terms of the source momentum (J_0) and buoyancy (B_0) fluxes as

$$l_M = \frac{Jo^{3/4}}{Bo^{1/2}} \tag{1}$$

for a three-dimensional buoyant jet and which represents the distance from the source within which momentum effects are dynamically significant and beyond which the dynamics are dominated by buoyancy. Therefore, when the value of the length scale l_M is high, the momentum flux (J_0) plays a dominant and destabilizing role on the buoyant jet, causing recirculating eddies or mixing over the entire water depth, while when the value of the l_M is low, the buoyancy flux (B_0) is the main and stabilizing element that fosters a stable field in which a buoyant surface layer is formed that does not communicate with the initial buoyant jet zone (Jirka *et al*., 1982). Furthermore, because an ambient cross flow existed in the direction of the channel, its momentum flux, defined as

$$J_a = S\, u_a^2 \tag{2}$$

where S is the transverse surface area of the ambient flow into the channel and u_a is the velocity of the cross flow, was taken into consideration, as destabilizing effect on the buoyant jet development. The values of these three parameters and the relations among them were considered to have a stable flow field; that is, a low value of the length scale l_M was planned so that buoyancy effects were comparable with momentum effects, and a low value of the cross flow momentum flux J_a was chosen so that the position of the free surface level and a cross flow velocity were as low as possible. In particular, for the experiments with a smooth bottom boundary, and with the source diameter D = 5 mm of the buoyant jet defined, the length scale l_M assumed values between

0.26 m and 0.44 m, whereas the values of the flow ambient momentum flux J_a was $7.5 \cdot 10^{-3}$ m^4/s^2 for all the experimental configurations. For the fresh water supply and its heating, a galvanized iron tank was used, which inside were four resistances of 12,500 W for the heating of the water till the fixed temperature (with maximum value 90°C), each one protected by a thermostat, and a temperature transducer for the water temperature measurement. A pump of 1 Hp, equipped with manometer and interception key, transferred the hot water from this supply reservoir to a second tank, positioned on a lifting platform, whose different levels were able to define the fixed source discharge. A comprehensive view of all of the buoyant jet generation system described is showed in Figure 2.

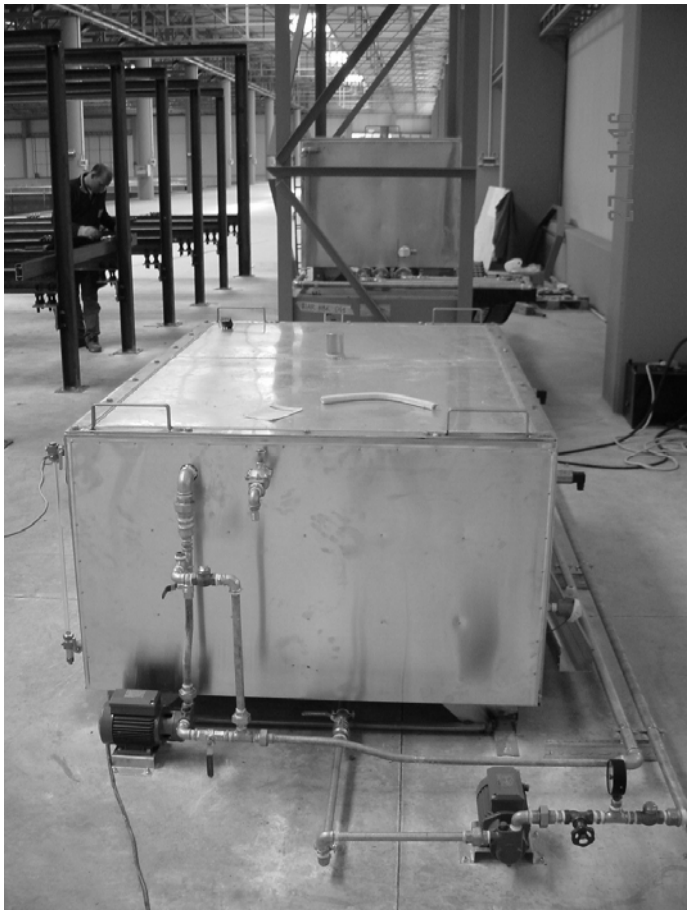

Figure 2. The tanks of the hydraulic circuit of the buoyant jet.

A Process Computer and a control software (which task was to store the test data and, if decided by the operator, to supervise all the system) was used to control and manage the buoyant jet system. It was able to generate the discharge of a flow with prefixed and constant pressure, flow rate and temperature into the channel described, and all of the facilities connected with the channel and the jet generation system.

To create a particular turbulence in the ambient cross flow, corrugated plastic elements were positioned on the bottom of the channel, forming a rough bottom boundary (Fig. 3). Three different kinds of roughness elements were used. The first one, was a roll of 10 m length and 3 m width, made of polyester resin strengthened with glass fiber, with a “wavelength" λ of 76 mm and an "amplitude" ε of 18 mm. A hole was made in the center longitudinal section, 6 m from the upstream channel section and 4 m from the downstream section, located in the trough of the bottom boundary “wave” surface. Each of the other kinds of corrugated elements used during the following experimental configurations, was formed by 11 panels of same dimensions, and with same material and technical characteristics of the previous kind, differing only by the values of λ and ε.

Experimental cases and conditions for vertical round buoyant jet issued in a cross flow with rough bottom boundary are listed in Table 1. In order to cover as wide a range of conditions as possible, experiments were conducted using several different values and combinations of the buoyant jet and bed-form parameters. Nevertheless, the experiments used the same working fluid (fresh tap water) throughout and the jet source diameter D was kept fixed (5.0 mm) for all runs. Different buoyant jet flow conditions were therefore created by changes in Q_0 and T_0. In particular, the jet temperature was changed for each configuration to have two fixed temperature differences $\Delta T = (T_a - T_0$, with T_a the ambient temperature) of 25°C and 35°C between the ambient and the jet. The first configuration provided a smooth flat bottom boundary, while the following three configurations have adopted the different panels with different values of the parameters λ and ε, described above. Eight different thermocouple sensors were utilised to measure the mixing of the heated water into the cross flow, with and without the rough bottom, whereas for the measurement of the velocity the ADV system was used, together with CollectV software for the data acquisition and ExploreV software for the data analysis, both of them products of Nortek, like the ADV.

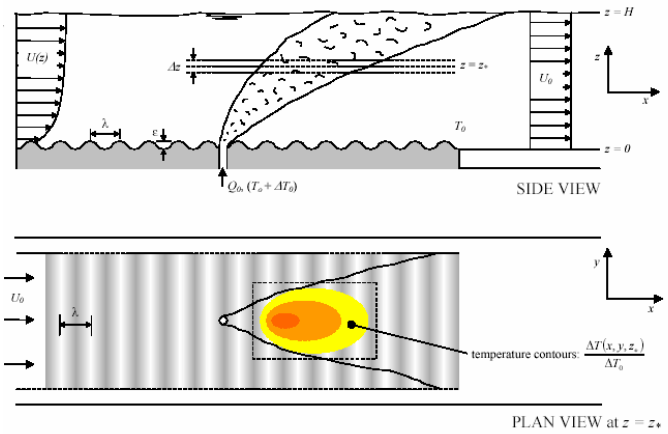

Figure 3. Schematic diagram of the experimental set up with corrugated plastic elements.

Table 1. Summary of experimental conditions.

Test	Q_0	H_a	Q_a	T_0	T_a	λ	ε
	l/s	m	l/s	°C	°C	mm	mm
T1	0.3	26	88	52	26	0	0
T2	0.3	26	88	62	27	0	0
T3	0.4	26	88	62	26	0	0
T4	0.4	26	88	52	27	0	0
T5	0.4	26	88	52	27	76	18
T6	0.4	26	88	61	29	76	18
T7	0.3	26	88	53	28	76	18
T8	0.3	26	88	60	25	76	18
T9	0.3	26	88	48	21	146	48
T10	0.3	26	88	54	18	146	48
T11	0.4	26	88	43	17	146	48
T12	0.4	26	88	53	19	146	48

2.2 *Laboratory results*

2.2.1 *Velocity field*

In order to study the turbulence effect upon the jet structure, a set of experiments was investigated with different configuration. The purpose of the experiment is to measure the three-velocity components (U, V, W) at different positions around the jet, where, U = mean stream-wise velocity, V = mean transverse velocity and W = mean vertical velocity, the measurement was determined by using an Acoustic Doppler Velocimeter (ADV). Figures 4-6 illustrate some of the experimental tests velocity vector map. It is to be noted that measurements shown in the three figures were made with the same channel discharge, the same source discharge and the same temperature excess at the source, the difference between theme being the nature of the channel bottom, which was a smooth surface bottom for Figure 4, corrugated surface bottom of "wavelength" λ = 76 mm and "amplitude" ε = 18 mm for Figure 5 and corrugated surface bottom of "wavelength" λ = 146 mm and "amplitude" ε = 48 mm for Figure 6.

The flow velocity vectors shown in those figures represent the mean velocity modules of the stream-wise and the vertical flow velocity components which were measured along the channel axes where y = 0.

As shown in Figures 4-6, it can be seen that the flow velocity vector directions and modules around the jet vary spatially. This variation is considered very rapid and more turbulent. Just for 1 or 2 cm in the upstream of the source, the velocity vectors keep the same direction along the vertical axes z and have a uniform distribution for the three bottom configurations.

Over the source nozzle and going toward the downstream end of the channel, the velocity vectors appear to have an upward moving flow area, through which they change their characteristics strongly.

Increasing the spatial coordinates (x, z), the velocity vectors for the three configurations change their characteristics step by step, reaching a uniform profile similar to that of the ambient flow.

The other hand, Figures 4-6 show that the ability of the jet to become more vertical depends upon the nature of the channel bottom. In the case when the channel bottom surface was smooth, the jet velocity vectors are deviated more toward the horizontal than the other configurations with the presence of a corrugated channel bottom surface. It can been seen that the velocity vectors direction are influenced by the "wavelength" λ and "amplitude" ε of the corrugated surface. When λ and ε increase the jet velocity vectors become more vertical. This is due to the fact that the jet is confined between the wave crests of the bottom.

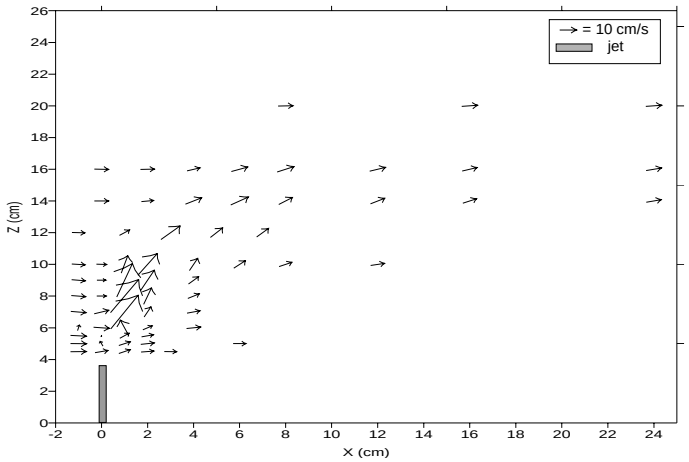

Figure 4. Near field velocity distribution for T1. Side view (Y = 0)

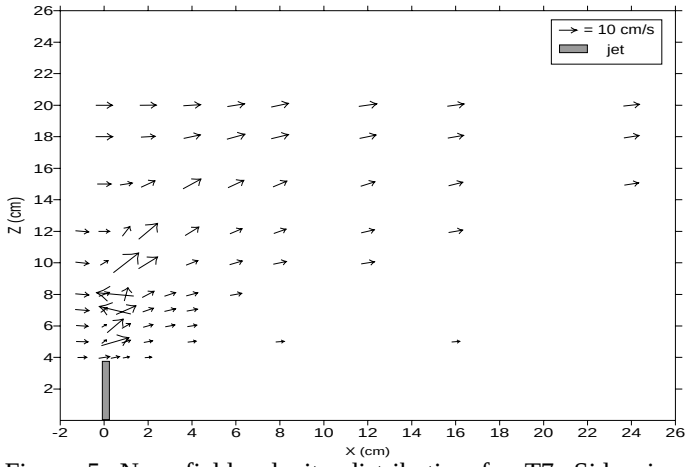

Figure 5. Near field velocity distribution for T7. Side view (Y = 0)

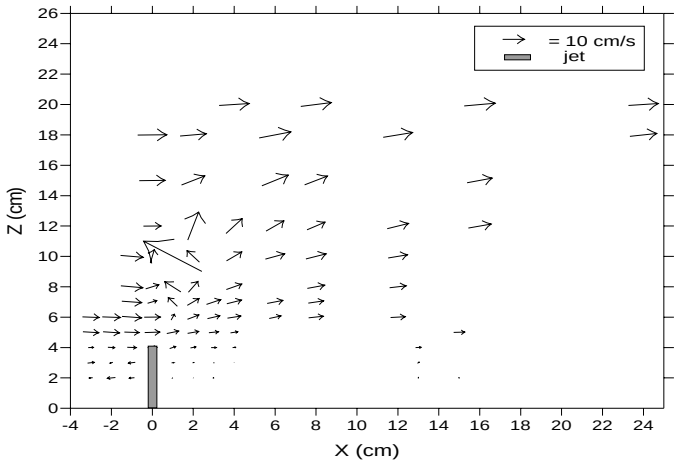

Figure 6. Near field velocity distribution for T9. Side view (Y = 0)

2.2.2 *Stress distribution*

As indicated in the previous paragraph, the channel bottom surface nature has a big effect upon the jet structure. In order to study this phenomenon in depth, a Reynolds stress analysis was established. As is well known, the statistical description of a turbulence flow starts by dividing the flow velocity into mean and fluctuating components. So, at each point the three instantaneous velocity components are written as:

$$u = U + u'$$
$$v = V + v'$$
$$w = W + w'$$

where u, v, w are the streamwise, transverse and vertical instantaneous flow velocity components, respectively, and *u'*, *v'* and *w'* are the streamwise, transverse and vertical flow velocity fluctuation components, respectively.

The quantities $u'v'$, $u'w'$ and $v'w'$ are the time-averaged streamwise-transverse, streamwise-vertical and transverse-vertical Reynolds shear stresses.

Figures 7-15 show a map of the Reynolds stresses in the x-z plan, with y = 0 cm, for Test 1, Test 7 and Test 9. Test 1 was a configuration with smooth surface channel bottom, Test 7 was a configuration with corrugated surface channel bottom of "wavelength" λ = 76 mm and "amplitude" ε = 18 mm, and Test 9 was a configuration of corrugated surface channel bottom of "wavelength" λ = 146 mm and "amplitude" ε = 48 mm.

From the figures, it is possible to highlight that the strong $u'v'$, $u'w'$ and $v'w'$ Reynolds stresses are present in the area localized near the jet source, where the velocity vectors change their characteristics strongly, as written in the previous paragraph. Furthermore, both positive and negative values of the Reynolds stresses were present in the same plan. In the measurement points far from the jet source, it was highlighted that the Reynolds shear stresses become small for all configurations. This is due to the small velocity fluctuations in these areas and the dominance of the cross flow velocity components with an absence of the jet stream effects.

Furthermore, one can see that there is a difference of the stress distribution between the analysed configurations, depending on the channel bottom surface. The absolute values of $u'v'$, $u'w'$ and $v'w'$ Reynolds shear stresses of the configuration with the smooth channel bottom are generally smaller than those of the other two configurations with corrugated channel bottom, as shown in table 2. The same table shows also that $u'w'$ Reynolds stress component of Test 9 is greater than the ones of Test 1 and Test 7. In addition, it can be seen that Test 9 shows a positive shear stress distribution larger than the negative one, as shown in Figure 12. On the contrary, the $v'w'$ Reynolds shear stress component is largely negative.

Examining the different figures, it can be seen clearly that the Reynolds shear stress distributions are more vertical when λ and ε increase.

Table 2. Reynolds stress values for test1, test7 and test9..

Test	u'v' (m^2/s^2)		u'w' (m^2/s^2)		v'w' (m^2/s^2)	
	min.	max.	min.	max.	min.	max.
T1	-60	220	-35	60	-80	0
T7	-120	220	-80	160	-220	20
T9	-60	180	-40	460	-80	20

2.2.3 *Temperature field*

In the present study, another aim was the measurements of the temperature field. The survey was run in a three-dimensional form, taking data at different levels and distances from the source orifice of the heated discharge.

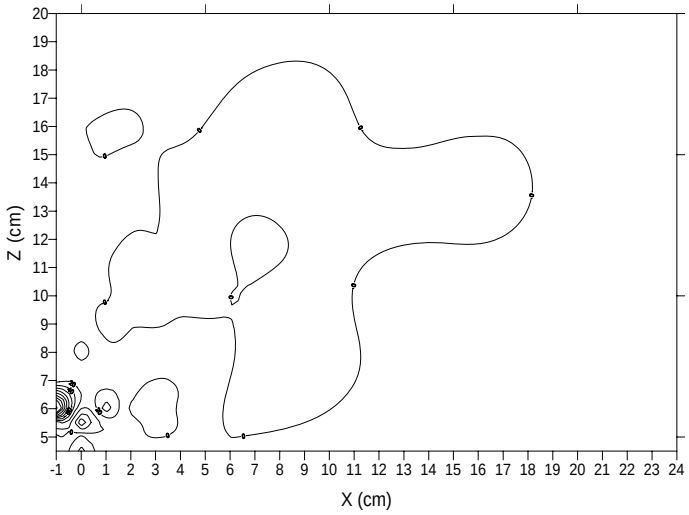

Figure 7. Streamwise-transverse (u'v') stress distribution for T1. Side view (Y=0).

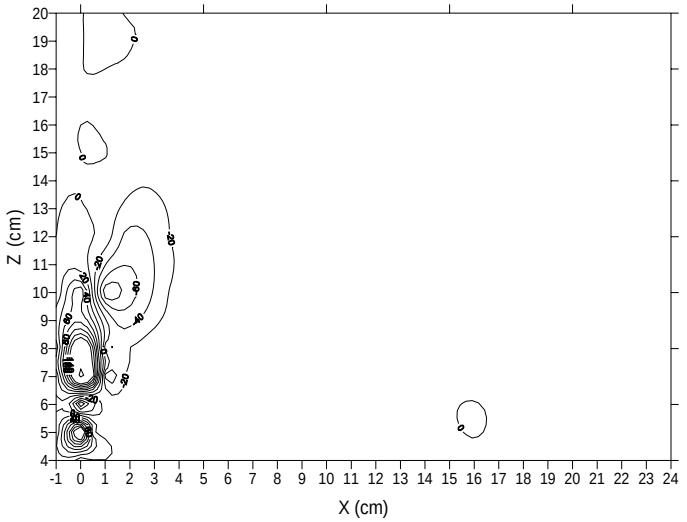

Figure 8. Streamwise-transverse (u'v') stress distribution for T7. Side view (Y=0).

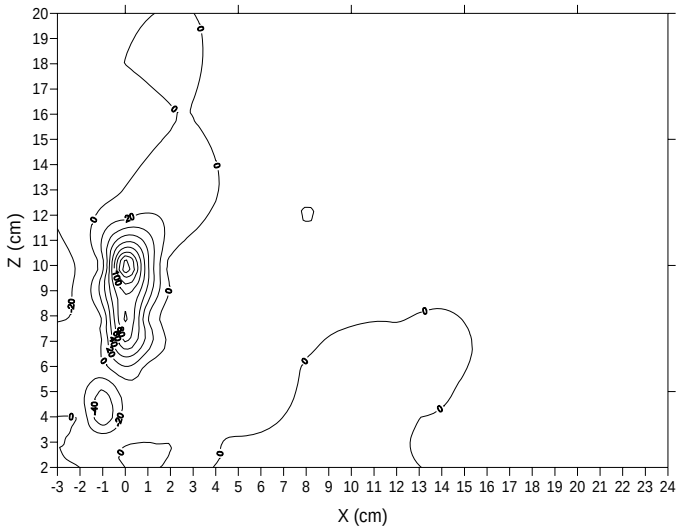

Figure 9. Streamwise-transverse (u'v') stress distribution for T9. Side view (Y=0).

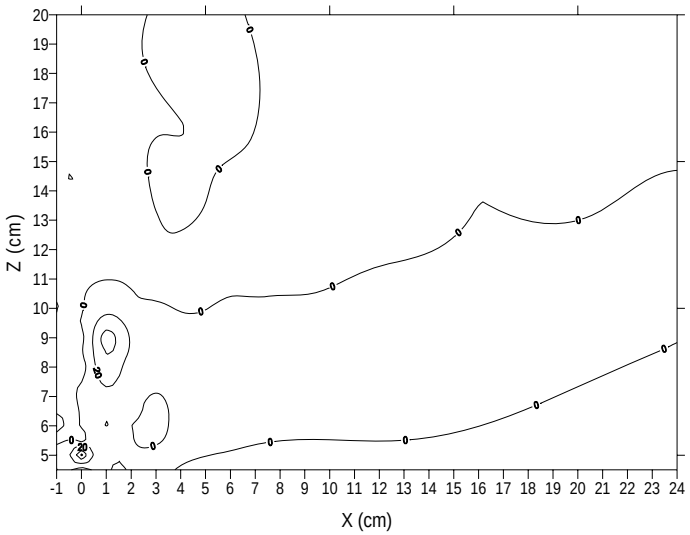

Figure 10. Streamwise-vertical (u'w') stress distribution for T1. Side view (Y=0).

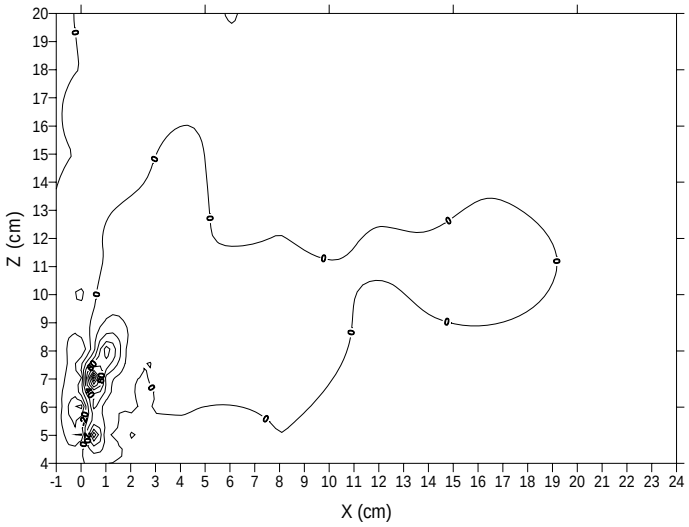

Figure 11. Streamwise-vertical (u'w') stress distribution for T7. Side view (Y=0).

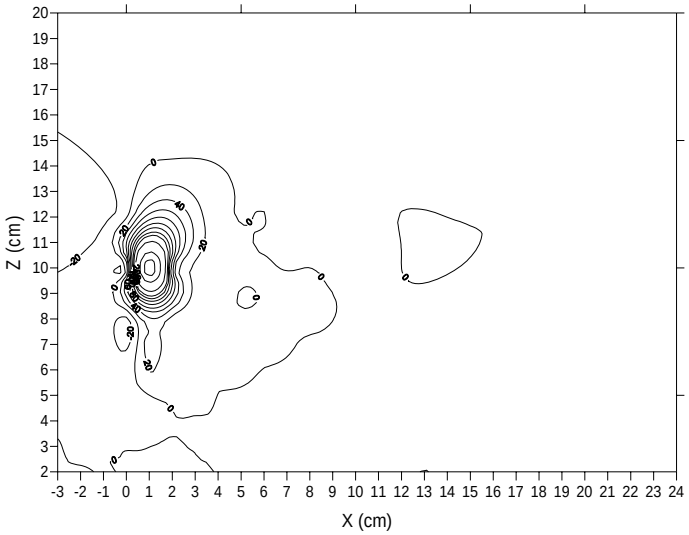

Figure 12. Streamwise-vertical (u'w') stress distribution for T9. Side view (Y=0).

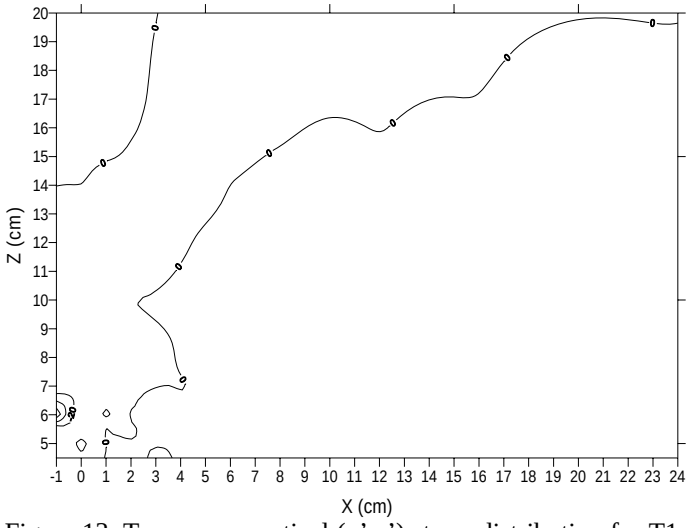

Figure 13. Transverse-vertical (v'w') stress distribution for T1. Side view (Y=0).

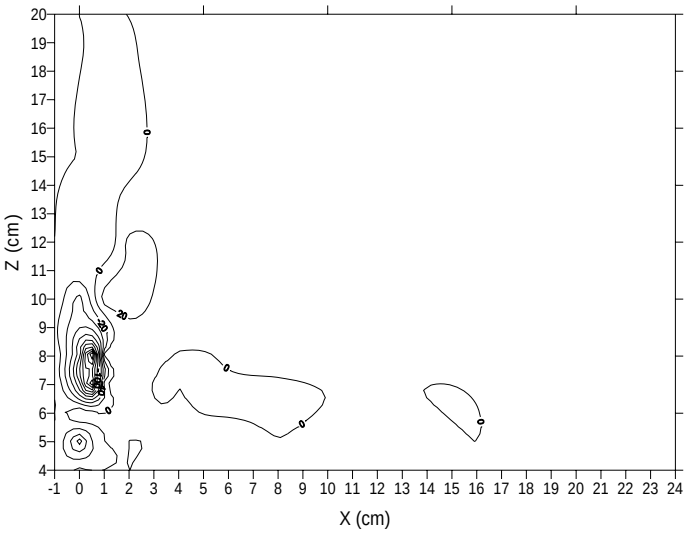

Figure 14. Transverse-vertical (v'w') stress distribution for T7. Side view (Y=0).

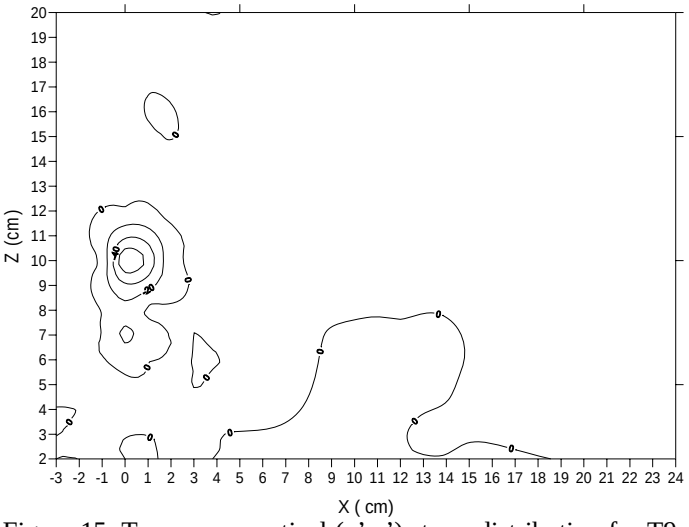

Figure 15. Transverse-vertical (v'w') stress distribution for T9. Side view (Y=0).

Among the twelve experimental cases, seven typical temperature profiles, at the centre longitudinal section of the channel, are shown in Figures 16-22. In these figures, the ratio $\Delta T/\Delta T_0$ is reported, where ΔT is the difference between the time-averaged temperature in the measurement point and the average ambient temperature, whereas ΔT_0 is the time-averaged excess temperature at the jet nozzle. In other words, this ratio represents the dilution of the buoyant jet into the cross flow. For the sake of brevity, Figures 16-22 were chosen taking into account (i) the three different bottom boundary conditions, which are smooth flat bottom, rough bottom with λ = 76 mm and ε = 18 mm, and rough bottom with λ = 146 mm and ε = 48 mm, and (ii) two different buoyant jets with different density, generated by different own temperatures, and different flow rates Q_0. The purpose is to show the different behaviour of the buoyant jet related to parameters such as λ and ε, and to its own characteristics. Attention was paid also to the horizontal distribution of the temperatures into the ambient, so the measurements were assessed also at different vertical layers.

The analysis of the figures show that the jet is more vertical (i.e. is less deviated towards the cross flow direction) in the case of rough bottom. Furthermore, the jet is less deviated in the case of rough bottom with higher values of λ and ε.

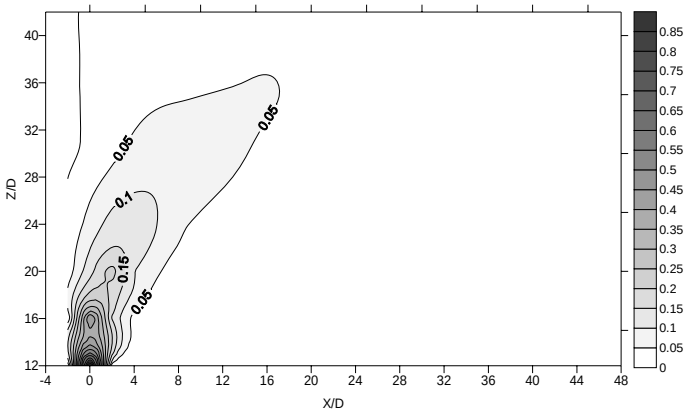

Figure 16. Longitudinal temperature distribution for Test 2.

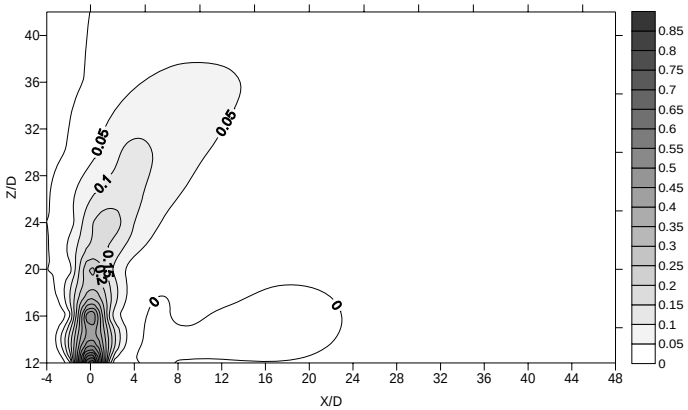

Figure 17. Longitudinal temperature distribution for Test 8.

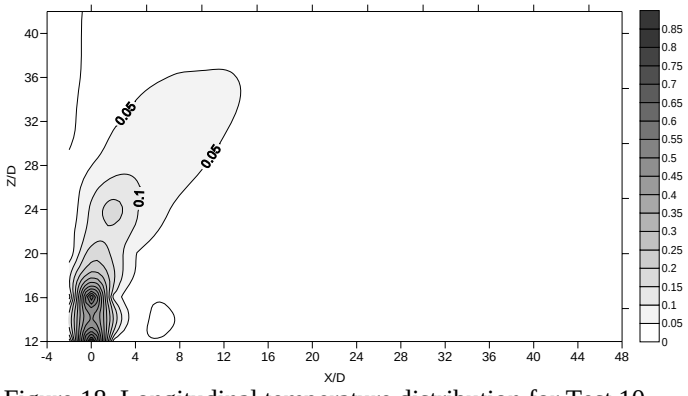

Figure 18. Longitudinal temperature distribution for Test 10.

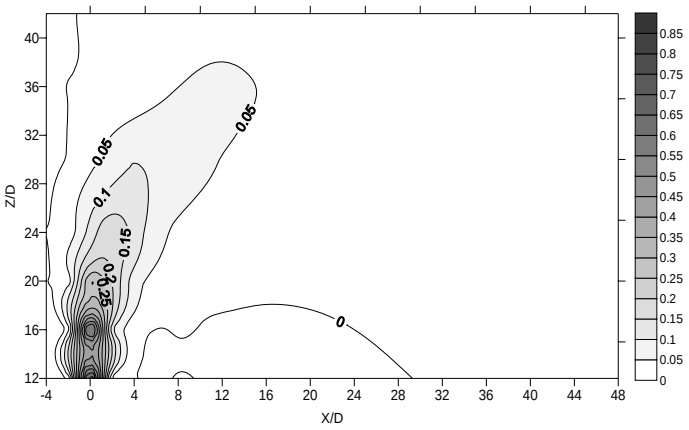

Figure 19. Longitudinal temperature distribution for Test 7.

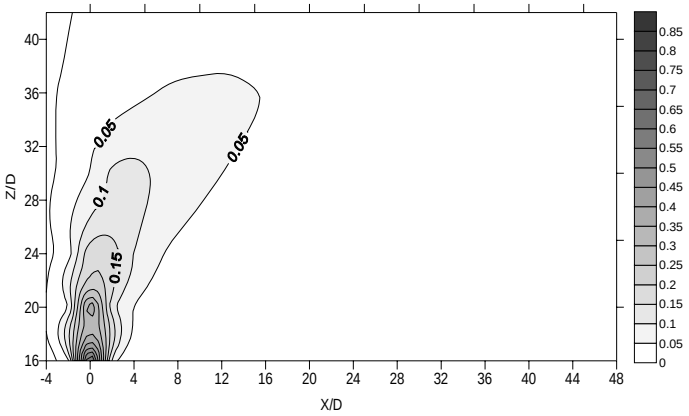

Figure 20. Longitudinal temperature distribution for Test 9.

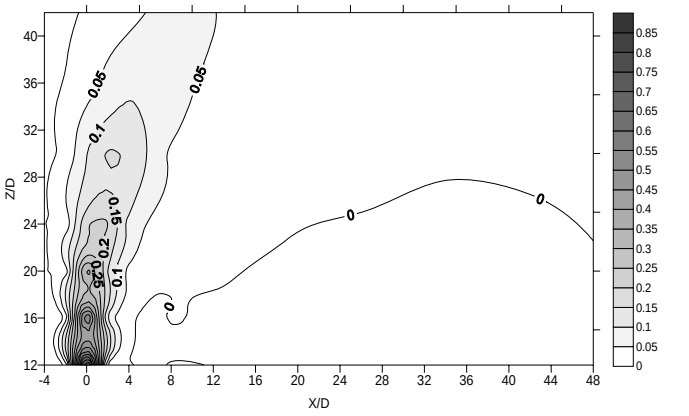

Figure 21. Longitudinal temperature distribution for Test 6.

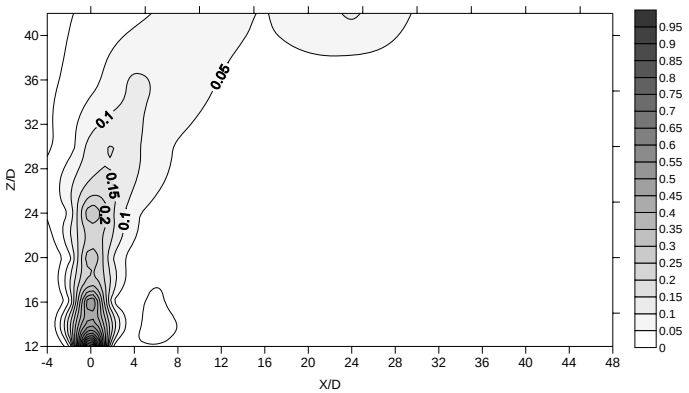

Figure 22. Longitudinal temperature distribution for Test 12.

3 CONCLUSIONS

Heated water mixing as the result of discharge from a submerged vertical round source located at the bottom of a channel was analysed, and the smooth and rough bottom boundary cases were compared. Several conclusions were attained from the analysis of the experimental data. Firstly, the experimental results reveal that the roughness elements on the bottom boundary affect significantly the trajectory of the buoyant jet. This result is clear from the figures of the longitudinal distributions of the dimensionless excess temperature. The comparison of the results enable us to highlight that the main effect of the roughness is to elevate the trajectory of the buoyant jet, which becomes more vertical. In addition, the kinematic generation by the roughness elements of a vertical component of the cross flow velocity seems to play an important role in this structural modification of the buoyant jet, as evidenced from the turbulence Reynolds stress distributions. Nevertheless, further work is required to establish and parameterise the relative role(s) of the relevant length scales of the flow and the topographic elements upon the structural modifications to the buoyant jet.

REFERENCES

Lee, J.H.W. 1984. Boundary effects on a submerged jet group. *J. of Engineering Mechanics*. ASCE, Vol. 122, No. 1:19-29.

Seo, I.W., Kim, H.S., Yu, D. & Kim, D.S. 2001. Performance of tee diffusers in shallow water with crossflow. *J. of Hydraulic Engineering*, ASCE, Vol. 127, No. 1:53-61.

Kim, Y.D., Seo, I.W., Kang, S.W. & Oh, B.C. 2002. Jet integral-particle tracking hybrid model for single buoyant jets. *J. of Hydraulic Engineering*, ASCE, Vol. 128, No. 8: 753-760.

Grass, A.J., Stuart, R.J. & Mansour-Tehrani, M. 1991. Vortical structures and coherent motion in turbulent flow over smooth and rough boundaries. Phil. Trans. Roy. Soc. London A336: 35-65.

Grass, A.J. & Mansour-Tehrani, M. 1996. Generalized scaling of coherent bursting structures in the near-wall region of turbulent flow over smooth and rough boundaries. Coherent Flow Structures in Open Channels (edit by Phil Ashworth, Sean Bennett, James L. Best, Stuart McLelland): 41-61.

Jirka, G.H., Doneker, R. L. & Hinton, S.W. 1982. User's manual for Cormix: A hydrodynamic mixing zone model and decision support system for pollutant discharges into surface waters. Defrees hydraulics laboratory, School of Civil and Environmental Engineering, Cornell University, Ithaca, New York.